CBERS-4 Satellite Thermal Design and Flight Model Environmental Thermal Tests

Rafael L. Costa[1] and Tiantian Wang[2]

National Institute for Space Research, São José dos Campos - SP, 12227-010, Brazil and Chinese Academy of Space Technology, Beijing, 100094, China

Valeri Vlassov[3]

National Institute for Space Research, São José dos Campos - SP, 12227-010, Brazil

and

Geng Liyin[4]

Chinese Academy of Space Technology, Beijing, 100094, China

The satellite CBERS-4 is the China-Brazil Earth Resources Satellite which was designed for remote sensing mission in Sun Synchronous orbit of 770 km of attitude. It consists of two modules, service and payload, thermally insulated from each other. The payload module is composed by four Earth imaging cameras, two developed by Brazil (INPE) and the other two by China (CAST). Thermal control is provided by the radiative insulation of external satellite surfaces with MLI blankets with radiator areas sized for the hottest orbital and operational conditions, either covered by OSR or white paint. For the cold case the safe heaters keep the camera optics and sensitive elements temperatures within their operation ranges. Some structural honeycomb panels were equipped with embedded and external two-core aluminum-ammonia heat pipes. This paper presents the satellite thermal design as well as the environmental thermal tests results. The satellite flight model was submitted to the combined thermal balance and cycle tests (TBT and TVT) that were conducted at the Space Center facilities of CAST in July-August 2014. Analysis of obtained data has demonstrated the design compliance to the thermal control subsystem requirements. The test setup is shown in detail from the thermocouples instrumentation to external heat fluxes simulation devices. In addition, a discussion is presented about Infrared Arrays (IRA) and the heat flux uniformity distribution as well as the radiometers positioning. Analysis of precision of specified external fluxes simulations with IRA during TBT is presented.

Nomenclature

AIT	=	Assembly, Integration and Test
BCHC	=	Battery Charge and Heater Controller
BDR	=	Battery Discharge Regulator
BOL	=	Beginning of Life
CAST	=	China Academy of Space Technology
CBERS	=	China-Brazil Earth Resources Satellite
DDR	=	Digital recorder Subsystem
EOL	=	End of Life
FM3	=	CBERS-3 Flight Model
FM4	=	CBERS-4 Flight Model

[1] Spacecraft Thermal Engineer, Space Mechanics and Control Division, rafael.costa@inpe.br
[2] Spacecraft Thermal Engineer, Thermal Department, wangtiantian.xjtu@gmail.com
[3] Spacecraft Thermal Engineer, Space Mechanics and Control Division, valeri.vlassov@inpe.br
[4] Spacecraft Thermal Engineer, Thermal Department, snikers@126.com

HP	=	Heat Pipe
INPE	=	National Institute for Space Research
IRA	=	Infrared Array
IRS	=	Infrared Imaging Camera
MC	=	Monte Carlo
MLI	=	Multilayer Insulation
MUX	=	Multispectral Camera
MWT	=	MUX & WFI Transmitter SS
OSR	=	Optical Solar Reflector
PAN	=	Panchromatic Multispectral Camera
PIT	=	PAN & IRS Transmitter SS
PM	=	Payload Module
SAG	=	Solar Array Generator
SM	=	Service Module
TBT	=	Thermal Balance Test
TCSS	=	Thermal Control Subsystem
TM	=	Thermal Model
TMM	=	Thermal Mathematical Model
TSLC	=	Taiyuan Satellite Launch Center
TVC	=	Thermal Vacuum Chamber
TVT	=	Thermal Vacuum Test
WFI	=	Wide Field Imaging Camera

I. Introduction

THE China-Brazil Earth Resources Satellite (CBERS) program is the result of an agreement signed back in 1988 between Brazil and China aiming at the cooperation and development of Earth remote sensing satellites,[1]. The National Institute for Space Research (INPE) is the responsible in the Brazilian side while the China Academy of Space Technology (CAST) is the Chinese counterpart. The CBERS-4, after CBERS-1, CBERS-2, CBERS-2B and CBERS-3, is the fifth satellite of CBERS program and it has exactly the same configuration of CBERS-3 wherein the cost and responsibility are equally distributed between the two countries. Since the CBERS-3 experienced a launch vehicle failure in December 2013 and was not put in orbit, a very fast Assembly Integration and Test (AIT) campaign was necessary and it was accomplished in less than one year, which was considered a remarkable achievement. The AIT of CBERS-4 was performed during 2014 at the CAST Space Center, in Beijing and successfully launched in December 2014 from the Taiyuan Satellite Launch Center (TSLC). This paper describes the satellite thermal design as well as the preparation, execution and results of the environmental thermal tests performed during the AIT campaign. From the thermal point of view, the Thermal Balance Test is the most important system test, because it gives the opportunity to verify the thermal design and its correct implementation, also its results are used to adjust and refine the Thermal Mathematical Model (TMM) that can be used to predict the satellite's thermal behavior under any conditions. Such TMM was correlated with the Thermal Model (TM) TBT results performed in 2009,[1]. The TBT for the flight model was performed mainly to verify the minor thermal design adjustments and their implementation accomplished Additionally, an analysis regarding the precision of specified external fluxes simulations with IRA during TBT is presented below.

II. Satellite Mission and Thermal Environment

The primary mission of the CBERS-4 is to image the surface of the Earth by the use of four cameras as the payload, the Multispectral Camera (MUX) and Wide Field Imaging Camera (WFI) are designed and built in Brazil. On the other hand, the Panchromatic Multispectral Camera (PAN) and Infrared Imaging Camera (IRS) are developed and built in China. The designed lifetime for the satellite is 3 years.

The orbit is sunsynchronous with an altitude of 770 km, 10:30 AM local time at the descending node, orbital period of ~100 minutes and 14 orbits per day.

For the orbital external heat fluxes, it is stated that the Solar constant may vary from 1323 to 1414 W/m², the Albedo from 0.38 to 0.46 and the IR Earth from 202 to 226 W/m²,[2,3].

Figure 1. Illustration of CBERS-4.

Along the orbit in nominal operation, the satellite is always poiting its +Z axis towards the Earth, which is the face where the four cameras are located, while the Solar Array Generator (SAG) is always tracking the Sun. Figure 1 illustrates the CBERS-4 satellite (without radiators).

III. Thermal Design

CBERS-4 Thermal Control Subsystem (TCSS) in under CAST responsibility, while INPE gives the necessary technical support and accompaniment.

The satellite is basically composed by a Service Module (SM) wherein all the fundamental subsystems are located, and a Payload Module (PM) which contains the four cameras, their transmitters (MWT and PIT) and the Digital recorder Subsystem (DDR). These two modules are thermally independent from each other since the interface has both conductive and radiative insulation by the use of insulating fiberglass washers and Multilayer Insulation (MLI) blankets, respectively. Thus, the TCSS considers the two modules separately for the thermal design and analysis purposes.

The thermal control is essentially based on passive means in order to have a more simple and reliable system and only uses active thermal control techniques when it is necessary.

For the radiative insulation, the satellite's body is all covered with 15-layered Multilayer Insulation (MLI) blankets, except the parts with radiators which are painted in S781 white paint for the faces with less solar incidence or covered with Optical Solar Reflector (OSR) for the areas with high solar incident fluxes, see Figure 2. The radiator sizes have been designed for the hottest thermal conditions, considering 3 years EOL material thermo-optical properties. All the internal surfaces of the side wall panels and electronic equipment external surfaces are painted with high emissivity paints in order to improve the radiation heat transfer between them, thereby minimizing internal temperature gradients. Electronic boxes with high dissipation are mounted on the panels with thermal interfiller materials, thermal grease (38 equipment) or indium foil (14 equipment), in order to minimize the thermal contact resistance. The main eligibility criteria between thermal grease and indium foil was the equipment placement; indium foil was used for equipment close to the optical instruments, such as star trackers and cameras due to its very low outgassing properties.

For the panels with large heat dissipation equipment, where additional heat transfer capability was needed, aluminum-ammonia axially grooved Heat Pipes (HP) were installed both embedded into the honeycomb panels and externally. Panels with HPs include battery panel, camera transmitters (MWT and PIT), Shunt, Battery Discharge Regulator (BDR) and Battery Charge and Heater Controller (BCHC).

Since the propulsion system is thermally sensitive, specially for low temperatures, all of its componets such as tanks, pipelines, filters and control valves have an active thermal control based
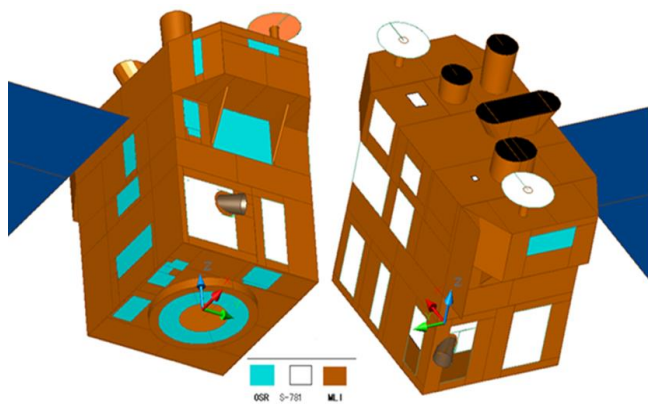

Figure 2. Schematic drawing of CBERS-4 external coatings (blue - OSR and white - paint).

on foil electrical heaters controlled by the Onboard Data Handling Subsystem (OBDH). Additionally, these components are thermally insulated from the satellite through the use of MLI blankets and insulating washers.

The Ni-Cd battery packs are also covered with MLI blankets and have their temperature controlled by electrical heaters. The infrared Earth sensors are also controlled by active heaters.

The cameras are thermally insulated from the rest of the satellite and have their own thermal control, which are based both on passive and active techniques. It is necessary because the cameras have very strict thermal control requirements, mainly because of the optical benches thermal distortion requirement.

IV. FM4 TBT/TVT Configuration and Setup

For the CBERS-4 Flight Model (FM4), the Thermal Balance Test (TBT) was performed in order to confirm and validate the TCSS, adjust the Thermal Mathematical Model (TMM) and confirm that thermal control parts have been implemented as designed. The TBT was conducted both to the CBERS 3&4 Thermal Model (TM), in 2009 and to the CBERS-3 Flight Model (FM3) in 2012. The TBT aims to put the satellite in the worst cold and hot conditions that it will face in orbit in order to verify the satellite thermal control design and implementation. The Thermal Vacuum Test (TVT) is always performed for flight models in order to exercise and test all subsystems in cold and hot conditions under vacuum, no matter how the temperatures are achieved.

For the FM4 TBT, 2 cases were considered as follows.

A. Thermal Balance Test (TBT) Case 1

It simulates the Cold conditions at the summer solstice, Solar Constant of 1323 W/m^2, Albedo of

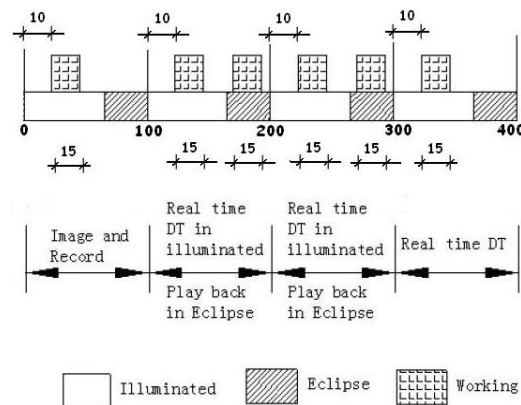**Figure 3. Orbit cycles – sunlight and eclipse times.**

0.38 and IR Earth of 202 W/m^2 . Thermo-optical properties of coatings are taken normal values in BOL. External heat fluxes are simulated as the average of the orbit period. Equipment at PM sare in stand-by condition. The SM equipment operats at their smallest heat dissipation mode, while the EPSS equipment are operating normally following the orbit cycles, Figure 3. Active thermal control of cameras, batteries, tanks and propulsion pipelines operates normally. Thruster internal heaters are ON.

Figure 4. 4-orbit profile – operating modes

B. Thermal Balance Test (TBT) Case 2

It simulates the Hot conditions at the winter solstice, Solar Constant of 1414 W/m^2, Albedo of 0.46 and IR Earth of 226 W/m^2. Thermo-optical properties of coatings, EOL values, considering 3 years of degradation have been taken into account in the evaluation of the simulated heat fluxes. SM equipment heat dissipation values are set according to operating modes. PM equipment and all cameras operate according to the diagram presented in Figure 4. Each cycle corresponds to 4 orbits; operation periods are of 15 min in sunlight (image and record) and 15 min in eclipse (playback). Each operation starts after 10 minutes when satellite enters eclipse or sunlight orbital phase, see Figure 4.
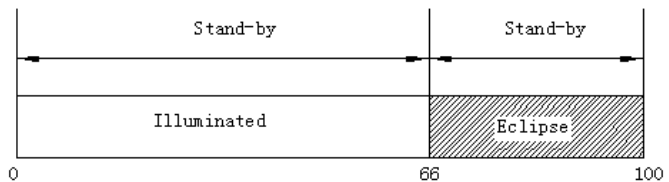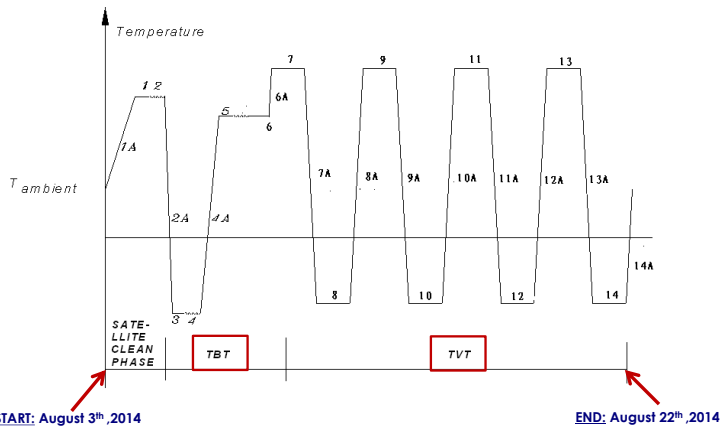
Figure 5. TBT/TVT test sequence.

START: August 3th ,2014

END: August 22th ,2014

C. Thermal Vacuum Test (TVT)

The TVT is not considered a test of the TCSS, because the temperatures are artificially imposed in order to test all satellite's subsystems performance through equipment functional tests in extremes of temperature[4]. This test is performed immediately after the TBT and is composed by 4 complete cycles of cold and hot levels based on TBT results. The TVT cold levels take the lowest temperatures of TBT Case 1

Figure 6. CBERS-4 average absorbed heat fluxes illustration – Thermal Desktop® TMM.

(cold) decreased at least by 5 °C, applied for the phases 8, 10, 12 and 14. On the other hand, the TVT hot levels take the highest temperatures of TBT Case 2 (hot) increased at least by 5 °C, applied for the phases 7, 9, 11 and 13. In both cases, acceptance temperature limits shall not be exceeded in order to preserve the equipment; Figure 5 shows the test sequence. For the cold and hot levels convergency, the temperature of 70 important equipment were observed until at least 80% reached the criteria.

Both for TBT and TVT, the satellite is at the flight configuration, except for the SAG and some antennas. All the MLI blankets and radiators are installed exactly as it will be in orbit. The satellite was instrumented with 289 T-type thermocouples in addition to the TCSS 126 telemetry thermistors.

The Thermal Vacuum Chamber (TVC) shroud temperatute was kept below -100 K (-173.15 °C) in order to simulate the deep space heat sink, also the TVC kept the pressure less than 1.3×10^{-3} Pa during the whole test.
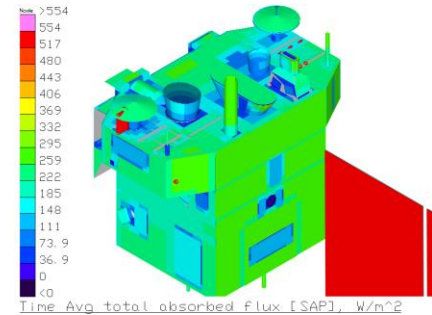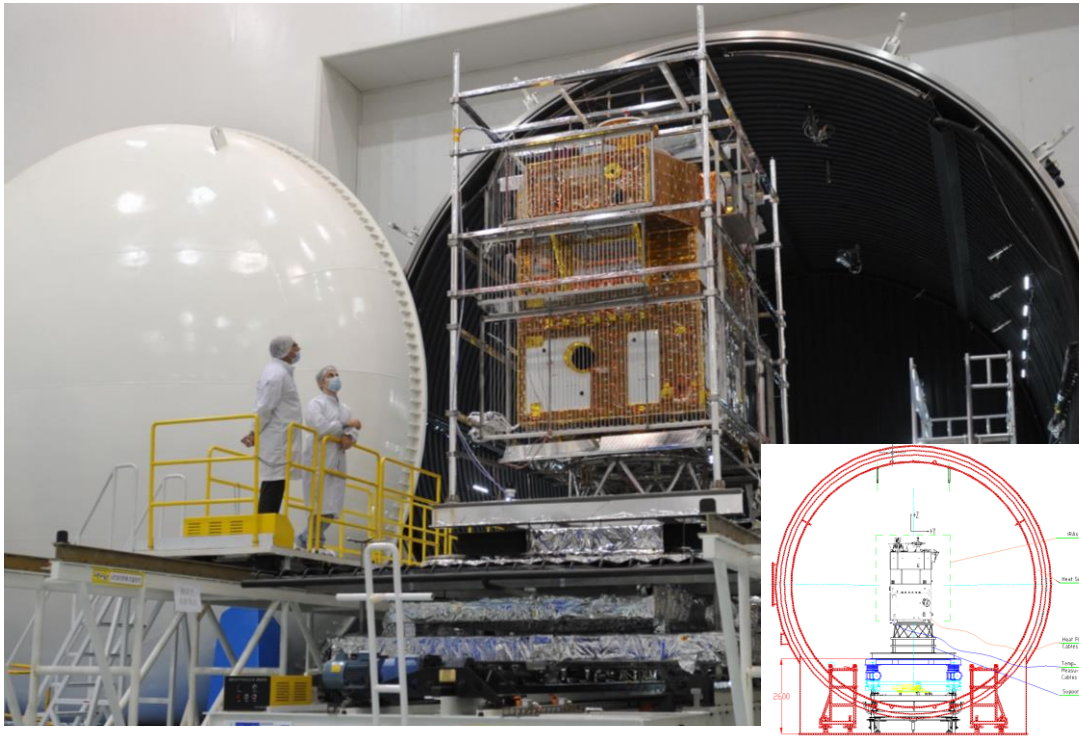
The TMM have been used to calculate the average absorbed heat fluxes from the combination of cold and hot conditions of in-orbit Direct Solar, Albedo and IR Earth over the MLI blankets, radiators and baffles. Figure 6 shows an illustration of the average absorbed heat fluxes obtained with a Thermal Desktop® TMM.

For the absorbed heat simulation, Kapton® foil heaters were applied directly over the MLI blankets surfaces (it has the same emissivity property as the MLI external layer surface). For the radiators and baffles heat flux simulation, Infrared Arrays (IRA) have been use with closed loop control based on radiometers monitoring temperatures. The IRA approach was used because it was easy and cheap to manufacture and is a well-known technique.

Figure 7 shows the FM4 at the final TBT/TVT configuration, moments before being placed into the TVC to start the test. Also, a schematic drawing of the test configuration is shown.

Figure 7. TBT/TBT FM4 final configuration and schematic drawing.

V. TBT/TVT Results

For the temperature monitoring, telemetry of all subsystems have been recorded and real-time monitored, including all TCSS temperature telemetries. Also, additional T-type thermocouples were installed throughout the satellite in order to better monitor the temperatures.

A. TBT Case 1 (cold)

For the cold case analysis purposes, it was considered the last four orbits of the Case 1, observing the maximum and minimum temperatures for the most important equipment, as shown in Figure 8. Also, the temperature maximum and minimum operating limits are plotted in the same chart.

As you can see, most of equipment has no variation of temperature because PM equipments are in stand-by condition.

At the SM, only few equipments of the EPSS, such as Shunt (RBDA), BDR (RBDB) and BCHC (RBDC) have periodical variations in temperature caused by change in heat dissipation due
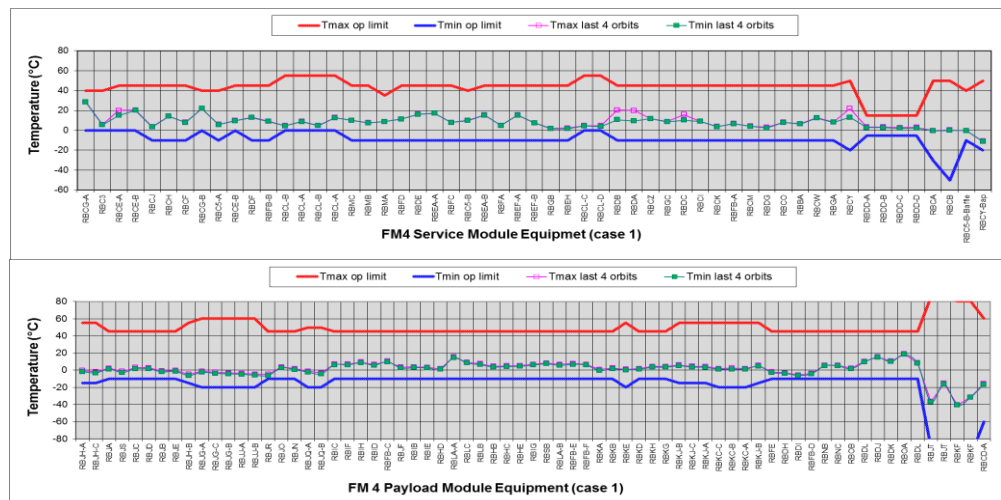

Figure 8. TBT Case 1 SM and PM equipment temperatures and their operational limits.

6

International Conference on Environmental Systems

to the sunlight/eclipse cycle.

It is very clear that all the equipment have their temperature within the operational limits; that means the thermal control has achieved its role for the cold case conditions.
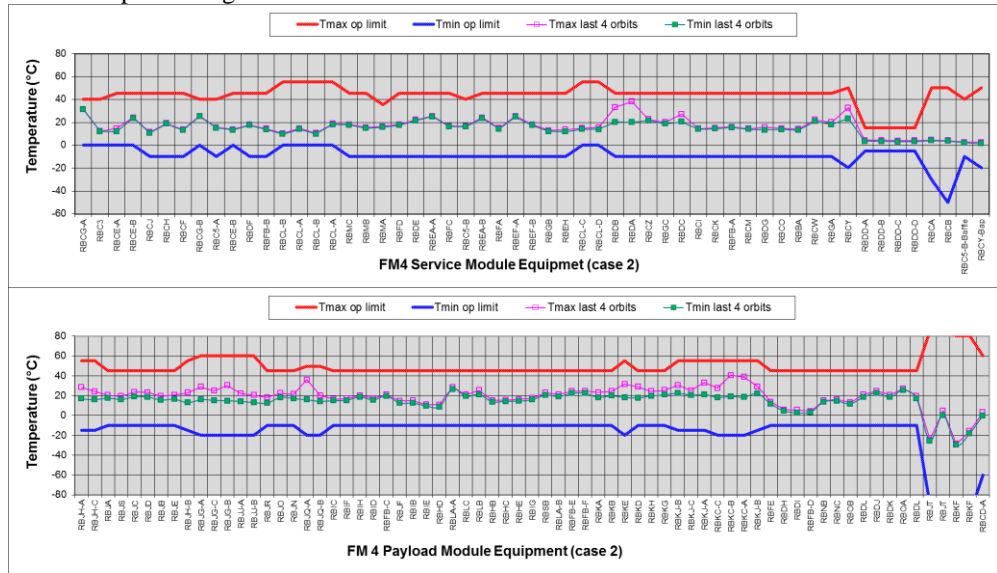
B. TBT Case 2 (hot)

Similarly, for the hot case analysis purposes, it was considered the last four orbits of the Case 2, observing the maximum and minimum temperatures for the most important equipment, see Figure 9. The maximum and minimum temperature operational limits are plotted together in the chart.

Differently from the cold case, many of the PM equipment have variations in temperature because they are turned ON and OFF according to their in-orbit operation modes, following the profile of Figure 4.

The SM equipment present the same behavior: only few equipments of the EPSS, such as Shunt (RBDA), BDR (RBDB) and BCHC (RBDC) have periodical variations

**Figure 9. TBT Case 2 SM and PM equipment temperatures and their operational limits.**

in temperature caused by change in heat dissipation due to the sunlight/eclipse cycle. Once again, one can see that the thermal control has done its job, it was able to keep all important SM and PM equipment within their operational temperature limits.

C. TVT

For the TVT cold levels, the temperature of the 70 most important equipment were monitored observing the target temperature, which was the minimum TBT temperature decreased at least by 5 °C The Figure 10 shows the chart of the maximum and minimum temperatures observed during the cold levels, the target for these levels and the minimum operational limit of each equipment.
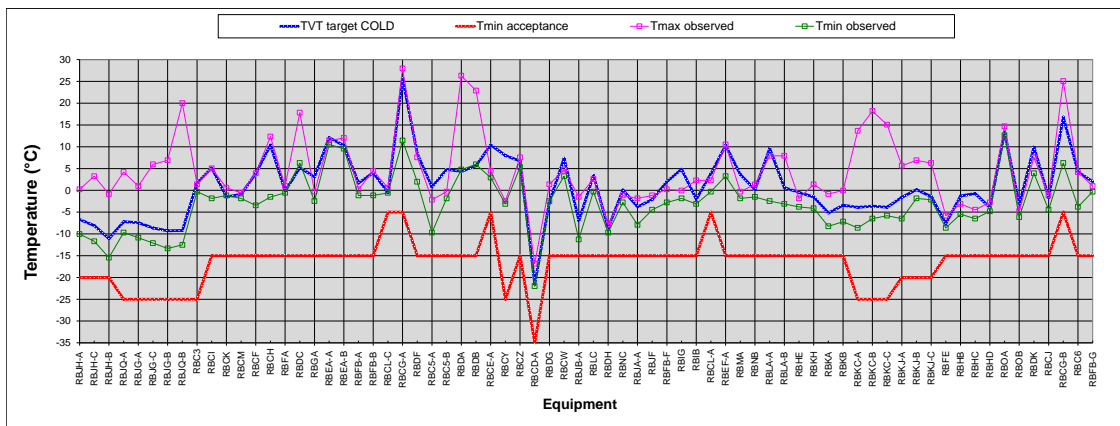
Figure 10. TVT cold levels temperatures – 70 important equipment.

It is important to note that during TVT cold levels, most of the equipment reached the target and none of them experienced temperatures below the operational acceptance limits.

Similarly, for the TVT hot levels, the temperature of the 70 most important equipment were monitored observing the target temperature, which was the maximum TBT temperature increased at least by 5 °C but never exceeding the
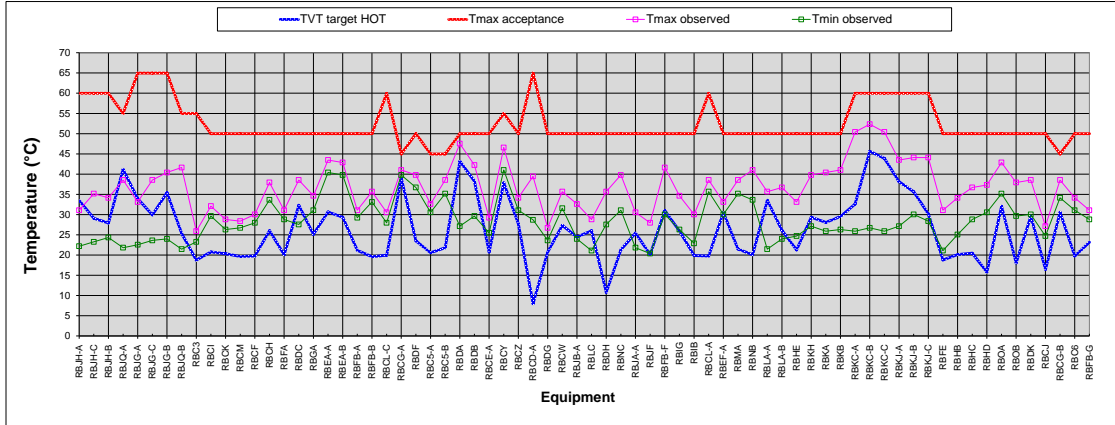

Figure 11. TVT hot levels temperatures – 70 important equipment.

maximum operational acceptance limits. The Figure 11 shows the chart of the maximum and minimum temperatures observed during the hot levels, the target for these levels and the maximum operational acceptance limit of each equipment. As required, more than 80% of equipment reached the target.

Functional tests of all subsystems were performed during cold and hot levels, observing performance parameters, and demonstrated that everything worked as expected.

VI. Infrared Array (IRA) Analysis

A. Flux uniformity

There is a concern about simulating external heat fluxes by the use of IRAs because in-orbit incident fluxes over the MLI and radiator surfaces are homogeneous, while the fluxes from IRA are not uniform. In order to have confidence that the test would provide equivalent conditions, the degree of non-uniformity of IRA flux shall be evaluated. To perform a rough evaluation of sensitivity of flux non-uniformity degree to the IRA main parameters, simplified analytical model can be used. The basic geometry consists of a set of infinite strips positioned over an infinite surface, as shown in Figure 12. Approximately, this geometry represents the radiative array and satellite radiator.
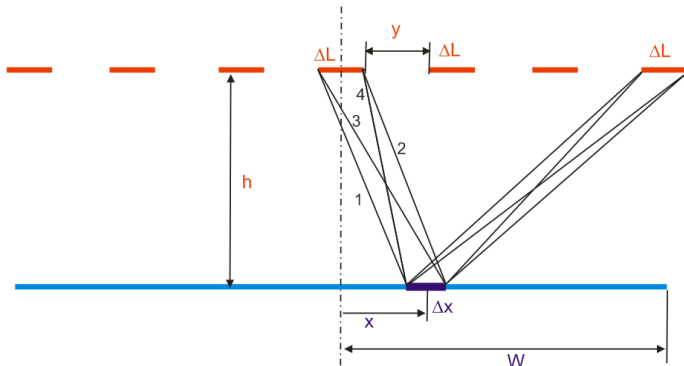

Figure 12. IRA conception uniformity analysis.

The basis for the nonuniformity of the incident flux from the IRA to the surface lies on the nonuniformity of the view factors distribution. The simplest way to build such a distribution function for the given geometry is to use the Crossed-string method to define the view factor from a strip ΔL to a small element of the surface Δx. Such a function for one IRA strip is defined through the equations below.

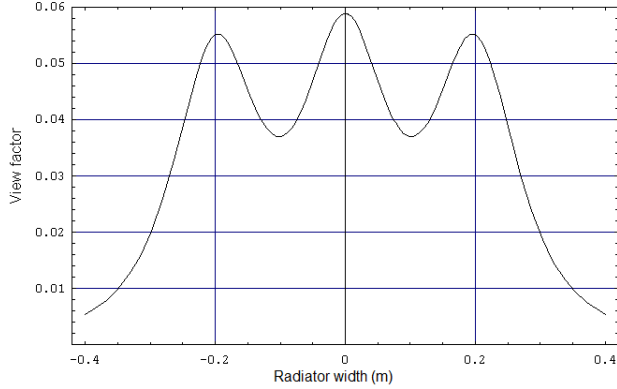$$L_1 = \sqrt{h^2 + (x - \Delta x/2 + \Delta L/2)^2}$$

$$L_2 = \sqrt{h^2 + (x + \Delta x/2 - \Delta L/2)^2}$$

$$L_3 = \sqrt{h^2 + (x + \Delta x/2 + \Delta L/2)^2}$$

$$L_4 = \sqrt{h^2 + (x - \Delta x/2 - \Delta L/2)^2} \qquad F_{\Delta L - \Delta x}(x, h) = \frac{L_3 + L_4 - L_1 - L_2}{2dL}$$

As an example let´s consider an IRA consisting of 3 strips positioned as the following: one at the center and two others at the edges of the W-wide radiator. For numerical values $\Delta L = \Delta x = 1$ cm, h=0.1 m, W=0.4 m, the view factor distribution is shown in the chart of Figure 13.

The chart also shows the illumination of neighbor area lying out of [-0.2,0.2] radiator dimension.

The view factor from the entire IRA of N strips to the surface is evaluated through the view factor algebra.

$$F_{IRA-\Delta x} = \frac{1}{N} \sum_{i=1}^{N} F_{\Delta L - \Delta x}(x + y_i, h)$$

$$F_{IRA-W} = \frac{1}{N\Delta x} \sum_{i=1}^{N} \int_{-W}^{W} F_{\Delta L - \Delta x}(x + y_i, h) dx$$

Figure 13. View factor distribution for the case of 3 strips IRA.

The view factor magnitude in this function depends of parameter of discretization Δx. However, once we want to evaluate the non-uniformity, the relative values will be used instead. The non-uniformity ΔF can be evaluated as a ratio between the maximum variations and the average view factor value.
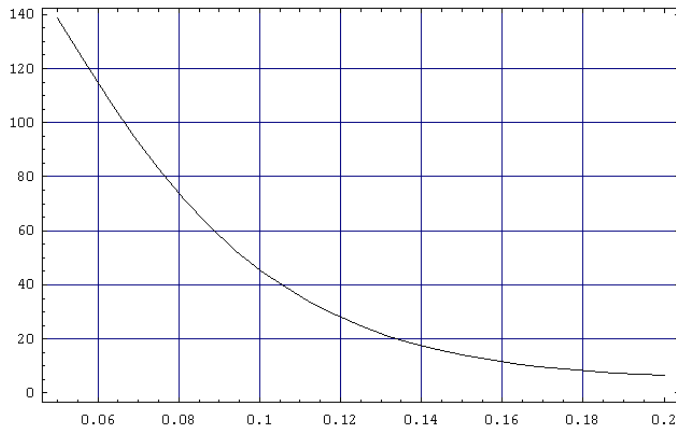
$$\Delta \overline{F}(h) = \frac{(F_{IRA-\Delta x}^{max}(h) - F_{IRA-\Delta x}^{min}(h))}{\overline{F}_{IRA-\Delta x}(h)} 100\%$$

Where

$$F_{IRA-\Delta x}(x, h) = \frac{1}{3}\left(F_{\Delta L - \Delta x}(x, h) + F_{\Delta L - \Delta x}(x - W, h) + F_{\Delta L - \Delta x}(x + W, h)\right)$$

$$F_{IRA-\Delta x}^{max}(h) = F_{IRA-\Delta x}(0, h); \qquad F_{IRA-\Delta x}^{min}(h) = F_{IRA-\Delta x}(W/2, h)$$

In this case the ΔF does not depend on Δx value and reflects the view factor maximal relative variation over the surface of *W* wide. For this example the non-uniformity is 45.6%.

The uniformity depends on the distance from the IRA to the surface. Figure 14 demonstrates how it changes for the given example when the distance varies from 5 cm to 20 cm.

However, it shall be noted that the more the distance, the more neighbor areas will be affected. Usually this effect is not desirable.

The analysis also shows that non-uniformity depends on the space between strips *y*: the less the space, the less non-uniformity.

For the present IRA configuration of CBERS satellite TBT/TVT test set-up, the space is about 5 cm and the IRA-surface distance is about 20 cm. These parameters yield the theoretical non-uniformity of about 2.4%.

Figure 14. Nonuniformity (in%) as a function of the distance from IRA to surface for the case of 3 strips.

B. IRA blockage

As presented above, decreasing the spacing between the strips yields the better flux homogeneity. On the other hand, such a dense arrangement increases the undesirable effect of blockage. The blockage reduces the view factor from the surface to TVC shroud and makes the

radiator surface temperature be slight higher under the same absorbed heat fluxes, specified from orbital conditions, if no corrections are applied.

The view factor from the surface to the TVC can be calculated from the IRA-to-surface view factor using the view factor algebra:

$$F_{W-TVC} = 1 - F_{W-IRA} = 1 - \frac{A_{IRA} F_{IRA-W}}{A_W}$$

Where A_{IRA} - is summary area of all IRA strips.

Effective blockage is correctly defined through the Gebhart factors. However, the blockage may not be even over the surface area. Figure 15 shows the view factor distribution from a surface to the TVC shroud, simulated to the case, when the main dimension of IRA and the surface are equal. The radiator surface dimension 0.6 x 0.3 m are picked from a typical part of IRA test layout of the CBERS-4 satellite.
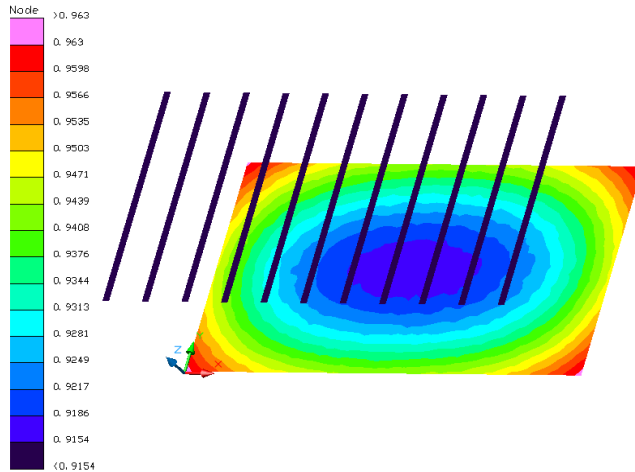
The simulation was performed using the following parameters: IRA strips wide-spacing: 1cm-5cm, IRA-surface distance is 20 cm; emissivity is 0.81 for the surface and 0.85 for the IRA strips. Number of rays per node in MC algorithm is 500000.

The simulation results show that the view factors vary between 0.907 and 0.959 (non-uniformity is 5.5%); and Gebhart factors to TVC vary in a similar way, from 0.915 to 0.963 (non-uniformity is 5.1%).

The better blockage uniformity can be achieved by decreasing the distance from IRA to the surface, however the flux non-uniformity will be increased. The blockage uniformity can be achieved also by increasing of IRA dimension (i.e. covering area), however the neighbor area will be also affected, that may be undesirable. In both cases the blockage factor tendency is to approach its limit magnitude 0.816, defined as follows.

Figure 15. Map of Gebhart factors from surface to TVC.

$$F_{W-TVC} \rightarrow 1 - \frac{A_{IRA}}{A_W}$$

When it is necessary to prevent the neighbor area to be affected, a shield can be installed. Figure 16 shows the maps of view and Gebhart factor distributions when a shield coated by polished aluminum foil (emissivity =0.1) is installed.
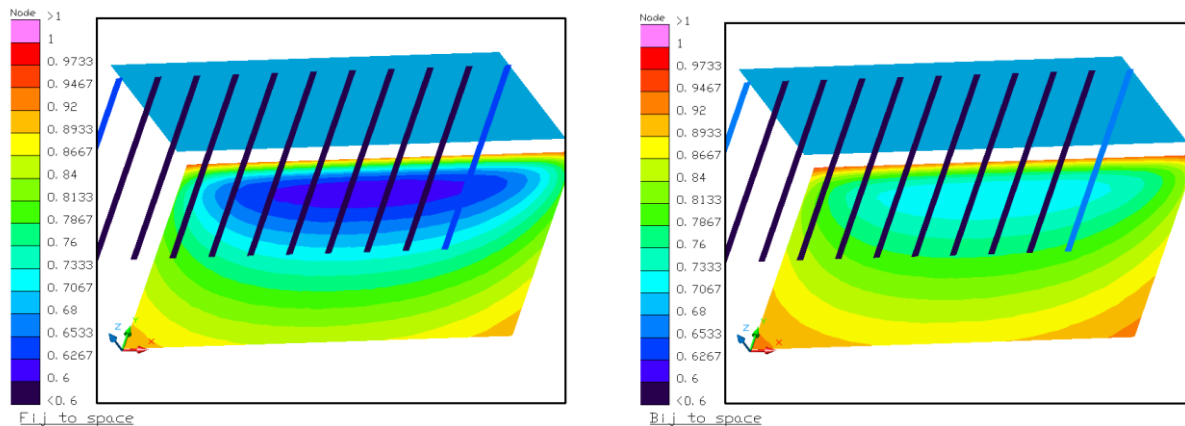

Figure 16. Map of view and Gebhart factors from surface to TVC

One can see, the shield installation yields the view factor over the surface to TVC to vary from 0.608 to 0.919 (non-uniformity is 40%), and the corresponding Gebhart factor varies from 0.711 to 0.935 (non-uniformity is 27%). Therefore the shielding prevents the neighbor areas from illumination, however the cost for this is the increasing of non-uniformity of the local heat balance and flux absorption.

C. IRA modeling

To correctly calculate the current needed on IRAs which correspond exactly the specified orbital absorbed fluxes, the simulation of test set-up of the satellite inside the TVC considering IRA geometries have to be performed by using a TMM. This TMM includes the full-size TMM of the satellite, TVC shroud, testing hardness and IRA set-up. The direct way to IRA simulation may be to represent of each strip of each IRA in the model. However, such approach becomes unfeasible due to high processing time needed, taking into account that such a fine geometry requires high number of rays setting in MC method. The alternative approach can be the IRA representation in the TMM as a semi-transparent solid plate.

The artificial transparency of such an IRA solid plate has to be set for both sides; the following formula works well:

$$\tau = \frac{\sum_{j=1}^{N_s} A_{sj}}{A_{IRA}}$$

The emissivity of the simulated semi-transparent plate is the same as the IRA strips emissivity, which is usually different for opposite sides, because the side facing the radiator is covered with high emissivity paint, and the opposite strip side has low emissivity to reduce the parasitic IRA flux to TVC shroud.

To prove the feasibility of the IRA modeling simplified approach, two similar models of the same assembly Surface-Shield-IRA have been created. For one of them, the IRA is represented as a set of strips and for the other, as a semitransparent plate. It is convenient to perform this parallel by comparison of the effect of IRA action to the surface in terms of temperature and heat fluxes between the elements of the assembling. To perform this, the surface is assumed to be a plate with artificially low (negligible) heat conductance. In this case each numerical element is insulated from neighbor elements, and its temperature would be a temperature of thermal equilibrium of the local balance of absorbed and emitted fluxes.

It is assumed the heat load over the surface is Q_{in}= 25 W uniformly distributed over the surface area (0.3 m x 0.6 m). The heat dissipation of IRA is 45 W. Figure 17 shows the temperature maps for two cases of IRA simulation.
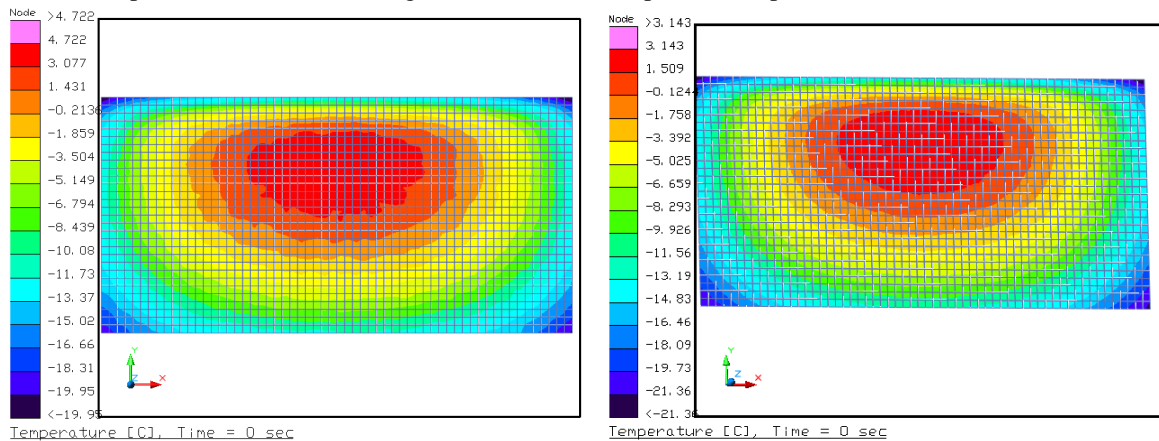
Figure 17. Temperature distribution over the surface when IRA is modeled as a set of strips and as a semitransparent plate

One can see, the results are similar within the tolerance of about 1.5 °C.

Table 1 shows the heat balance between the elements of the assembly for two cases of IRA modeling

Table 1. Heat balance components (case Qin=25; Q_IRA=45W).

	IRA TMM as a set of strips; $Qi{\to}j$(W)	IRA TMM as semitransparent plate; $Qi{\to}j$ (W)	$\Delta Q/Q$ (%)
SURFACE-to-TVC	37.37	36.15	3.3
SURFACE-to-IRA	-12.80	-11.57	9.6
SURFACE-to-SHIELD	0.426	0.419	1.6
IRA-to-TVC	26.45	27.69	4.7
IRA-to-SHIELD	0.750	0.737	1.7

It was found that for the present CBERS-4 thermal design such tolerance is acceptable and lies within the usual precision of radiation calculations between the satellite elements and external fluxes. Therefore, the IRAs were simulated by a simplified approach as semitransparent plates.
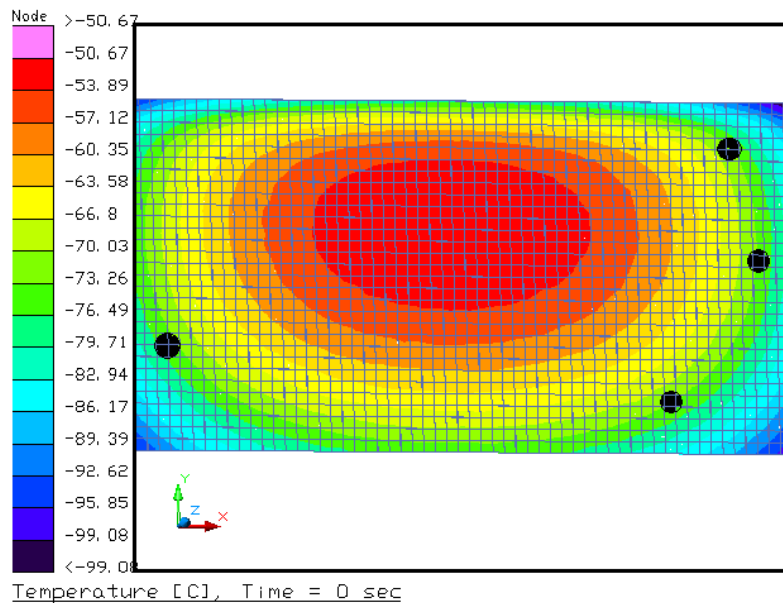
D. Radiometer positioning

During the test, radiometers are used to control the IRA electric current in a closed loop system. Assuming the flux absorbed by the radiometer and the surface is the same, this is an effective way to control IRA current without considering the complex problem of radiative heat transfer of the satellite in the TVC taking into account IRA layout and parameters. The IRAs are controlled through the feedback of radiometer target temperature that is a function of the absorbed flux

$$q_{abs} = \sigma \varepsilon_r T_r^4$$

However, the effects of non-uniformity in the blockage and in absorbed heat flux can affect the precision of IRA current control. In general, the non-uniformity does not affect the thermal balance of radiator surfaces, once the average flux is preserved, taking into account that usually radiator surfaces have sufficient spatial effective conductivity, of order of 6 to 9 W/m/K for honeycomb structural panels, that can smooth the temperature effects due to absorbed fluxes non-uniformity. Yet, it should be careful when selecting the radiometer position, because if the non-uniformity effects are not considered, it can lead to an erroneous signal of the radiometer.

To illustrate this, we consider the radiometers having the same emissivity as the satellite radiator surface, $\varepsilon_r= 0.85$. We can use the same IRA assembly, containing IRA and shields. We also assume the surface in the model as a plane above the radiator surface where a radiometer can be installed. Remember, that the surface does not have in-plane thermal conduction, so it serves rather as control plane. Under the same IRA heat power ($Q_{IRA}= 45$ W and $Q_{in}= 0$ W), the temperature distribution over this control surface (where radiometer can be installed) is shown in Figure 18.

Figure 18. Possible positions of the radiometer for the given example

One can see, the target temperature varies from -50.7 to -99.1 °C. The average absorbed heat flux is 74.7 W/m^2 that corresponds to average temperature of -74.8 °C; Therefore, the possible positions of the radiometer location shall be selected in the positions where the target temperature of radiometer is equal to the average temperature. In the figure some such points are marked in black.

All revealed analyzes were considered during thermal project of TBT set-up.

VII. Conclusion

All the required environmental thermal tests (TBT and TVT) were conducted according to the specification. It was presented an overview on the CBERS-4 thermal design and configuration. Also, it was shown a general view of the tests preparation and execution. The test results are considered to be consistent and reliable. According to the TBT results, all requirements related to the TCSS subsystem were complied and it was demonstrated that the thermal control is performing its function satisfactorily. That provides strong evidences that the thermal design is correct and it was well implemented, which gives confidence that the TCSS will play its role in orbit. TVT results show that none of the selected important equipment have ever exceeded the acceptance temperature limits and all subsystems performed well on their functional tests, under the cold and hot test conditions. It was presented an analysis of IRA approach used to simulate external heat fluxes over the satellite.

References

[1]Leite, R., Guoqiang, L., Vlassov, V., Liyin, G., Rivas, G. A. R., Entao, C., Bin, W., "CBERS 3&4 TM Thermal Balance Test Results and Satellite Thermal Mathematical Model Correlation," *Proceedings of the 44th International Conference on Environmental Systems – ICES*, 2010, pp. 1-8.

[2] D.G.Gilmore. Satellite Thermal Control Handbook. The Aerospace Corporation, 1994.

[3] Space engineering: Space environment. ECSS-E-10-04A, 21 January 2000.

[4] Space engineering: Testing. ECSS-E-10-03A. 15 February 2002. .